Research Article | Vol. 27, No. 24 / 25 November 2019 / Optics Express 35903
Optics EXPRESS

Underwater superoleophobic and anti-oil microlens array prepared by combing femtosecond laser wet etching and direct writing techniques

MINJING LI,[1,2] QING YANG,[1,2,5] JIALE YONG,[2,3] JIE LIANG,[2,3] YAO FANG,[2,3] HAO BIAN,[2,3] XUN HOU,[2] AND FENG CHEN[2,3,4]

[1]School of Mechanical Engineering, Xi'an Jiaotong University, Xi'an 710049, China
[2]The International Joint Research Laboratory for Micro/Nano Manufacturing and Measurement Technologies, Xi'an Jiaotong University, Xi'an 710049, China
[3]State Key Laboratory for Manufacturing System Engineering and Shaanxi Key Laboratory of Photonics Technology for Information, School of Electronics & Information Engineering, Xi'an Jiaotong University, Xi'an 710049, China
[4]chenfeng@mail.xjtu.edu.cn
[5]yangqing@mail.xjtu.edu.cn

Abstract: As an important micro-optical device, microlens array (MLA) also has broad applications in aqueous environment apart from atmosphere, such as bioscience research, ocean exploration, and microfluidic systems. However, the surface of the normal MLA is easily polluted by oil contaminations when the MLA is practically applied in a water medium, leading to the loss of its optical imaging ability. Herein, we fabricated a functional MLA with underwater anti-oil and self-cleaning abilities by combining the femtosecond laser wet etching (FLWE) and the femtosecond laser direct writing (FLDW) techniques. The as-prepared close-packed MLA is composed of 10000 single microlenses with the aperture diameter of 50 μm. The surface of each microlens is further textured with micro/nanoparticles. Clear and uniform images could be captured by using the resultant MLA in water, demonstrating great underwater imaging ability. The modulation transfer function value is larger than 0.6 at 55 lp/mm. In addition, the micro/nanostructures endow the as-fabricated MLA surface with underwater superoleophobicity and oil-repellent performance. Various oils can be repelled by the resultant MLA in water. Underwater 1,2-dichloroethane oil droplet on the textured MLA has a contact angle of 158.0 ± 0.5° and a sliding angle of 2.0 ± 0.2°. The underwater superoleophobic MLA also has good mechanical durability. The anti-oil and self-cleaning functions will broaden the applications of the MLA in ocean exploration, bioscience research, microfluidic system, and many underwater MLA-based systems.

1. Introduction

As an important miniaturized optical component, microlens array (MLA) is widely applied in the three-dimensional imaging, protein detection, light homogenization, wavefront sensing, lab-on-a-chip devices, and microfabrication, because of its great imaging and light-field-regulation capabilities [1–7]. However, the traditional MLAs are easily polluted by oil contaminations when they work in water medium, which may lead to the loss of their imaging ability. Usually, various detergents and organic solvents are used to clean them, but these chemical substances will pollute our living environment. Moreover, the MLA-based component must be dismantled from the device to wash off the adhered oil contaminations. The waste of time for reparation also leads to a large economic loss. Therefore, it is an imperative demand for developing a new method to

#378177 https://doi.org/10.1364/OE.27.035903
Journal © 2019 Received 20 Sep 2019; revised 8 Nov 2019; accepted 11 Nov 2019; published 21 Nov 2019

Optics EXPRESS

fabricate a multifunctional MLA which synchronously has high optical performance, anti-oil, and self-cleaning abilities.

Nature gives us much inspiration to produce anti-oil surfaces such as superoleophobic surfaces [8–13]. Fish scales have great underwater superoleophobicity, on which the underwater oil droplet has a contact angle larger than 150° [14–15]. The anti-oil ability enables fish to keep its skin clean even in the oil-polluted water medium. Jiang et al. found that the underwater superoleophobicity of fish scales surface is derived from the hydrophilic chemical component and micro/nanoscale hierarchical structures [16]. Until now, a large number of studies have been focused on fabricating artificial underwater superoleophobic surfaces based on an oil/water/solid three-phase system [11,17–34]. For example, Jiang et al. obtained micro/nanoscale structures with underwater superoleophobicity on a silicon substrate by lithography etching [16]. Liu et al. fabricated textured copper oxide coating on a copper sheet by simple chemical etching in ammonia solution [17]. The as-prepared surface exhibits underwater superoleophobicity. Zhang et al. prepared underwater superoleophobic Ni/NiO surfaces with controllable oil-adhesion by electrochemical deposition and subsequent annealing process [18]. These resultant underwater superoleophobic surfaces have the capacity of anti-oil, underwater self-cleaning, and oil/water separation. Nevertheless, to the best of our knowledge, an underwater superoleophobic and self-cleaning MLA has rarely been reported, and the integration of excellent imaging ability and anti-oil function for a MLA still remains a great challenge.

Here, we report a novel way to prepare underwater superoleophobic MLA. Femtosecond laser wet etching (FLWE) technique was firstly applied to fabricate a normal MLA with smooth surface. Then, micro/nanoscale hierarchical structures were further created on each microlens surface by femtosecond laser direct writing (FLDW) treatment. The optical imaging performance and the modulation transfer function (MTF) of the resultant MLA demonstrate that the MLA possesses good imaging ability in water. In addition, the surface micro/nanostructures endow the MLA with underwater superoleophobicity, so the resultant MLA has excellent underwater anti-oil and self-cleaning abilities. The oil residue on the MLA surface can be easily cleaned away by water.

2. Experimental

2.1. Fabrication of smooth MLA

Commercial K9 glass (10×10×1.5 mm^3) was used as the substrate material. The laser beam (central wavelength = 800 nm, pulse duration = 50 fs, and repetition rate = 1000 Hz) was generated from a regenerative amplified Ti: sapphire laser system (Coherent Libra-usp-he) and was focused onto the glass surface by an objective lens (50×, NA = 0.60, Nikon), as shown in Fig. 1(a). The glass surface was irradiated by the laser via the point-by-point manner, resulting in an array of ablated craters. Every crater was ablated by 300 laser pulses with the power of 5 μJ. The distance between the adjacent craters was set at the constant value of 50 μm (Fig. 1(d)). After the laser irradiation, the glass sheet with original craters was immersed in the 10% hydrofluoric (HF) acid at room temperature (Fig. 1(b)). Subsequently, the concave MLA will be formed by selectively etching laser-modified region (Fig. 1(e)). The details of the formation principle of the MLA is reported in our previous articles [35,36].

2.2. Generation of micro/nanostructures on MLA surface

Femtosecond laser has been demonstrated to be an effective tool to fabricate micro/nanostructures [37,38]. As shown in Fig. 1(c), the laser beam was focused on the surface of the as-prepared smooth MLA again by an objective lens (20×, NA = 0.40, Nikon). The line-by-line scanning method was used to produce hierarchical micro/nanoscale structures on the MLA surface (Fig. 1(f)). The laser power was set at 10 mW. The average distance (*AD*) between the adjacent irradiated points was adjusted by controlling the laser scanning speed and the scanning interval.

Optics EXPRESS

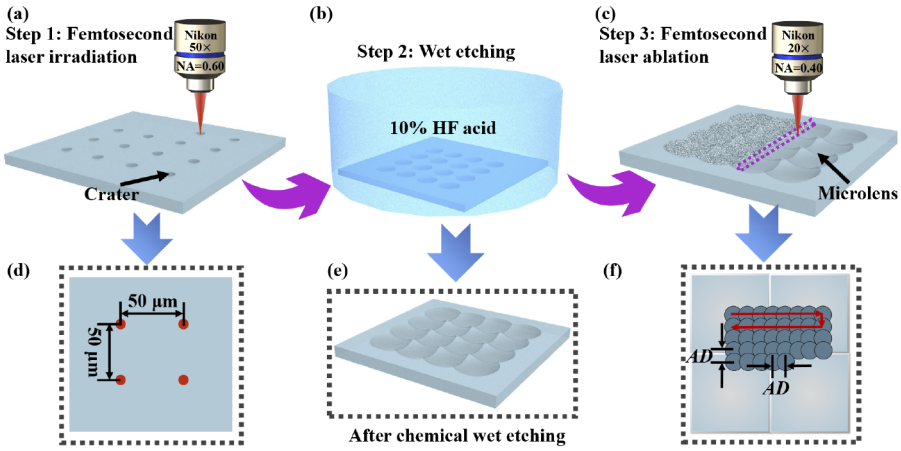

Fig. 1. Fabrication process of micro/nano-structured MLA. (a,d) An array of ablated craters was formed by femtosecond laser irradiation. (b,e) Chemical etching process for forming normal MLA. (c,f) Micro/nanoscale structures were generated on the MLA surface via femtosecond laser ablation.

2.3. Characterization

The surface topography of the MLAs was observed through a scanning electron microscope (FlexSEM1000, HITACHI, Japan) and a laser confocal scanning microscope (LEXT-OLS4000, Olympus, Japan). The optical performance of the resultant MLA was investigated by an optical system which contains a microscope (Nikon, Japan) and a charge-coupled device (CCD). The optical transmission spectrum at the wavelength of 400 ~ 800 nm was tested by a spectrophotometer (UV 3010, Hitachi, Japan). The wettability of an underwater oil droplet (10 μL) on different types of MLA surfaces was measured by a contact angle system (JC2000D, Powereach, China). Generally, 1,2-dichloroethane was adopted as the main test oil for investigating underwater oil wettability because its density is higher than that of water. The average contact angle and sliding angle values were obtained by measuring the sample at five different positions.

3. Results and discussion

3.1. Surface morphology

An array of microlenses was firstly created on the glass surface by FLWE method, as shown in Figs. 2(a) and 2(b). The surface of the microlens is smooth and there are no noticeable particles on the original MLA (Fig. 2(b)). After subsequent FLDW treatment, micro/nanostructures were further induced on the MLA surface because of laser ablation (Fig. 2(b)). The surface of the resultant microlens is completely decorated with micro-bumps which are about 1 μm in size. Such micro/nanostructures were generated by the laser-matter interaction during laser ablation. Figure 2(d) depicts the three-dimensional (3D) profile of the textured MLA. Although the microlens is decorated with micro/nanoscale structures, the microlens still maintains its curved surface profile. The result shows that the average aperture diameter (D) and height (h) of the microlens are 49.98 μm and 8.04 μm, respectively. The focal length (f) and the numerical aperture (NA) of the MLA can be calculated by the following formulas [36,39]:

$$f = \frac{h^2 + r^2}{2h(n-1)} \tag{1}$$

$$NA = \frac{D}{2f} \tag{2}$$

Optics EXPRESS

where r is the radius of the microlens which is equals to $D/2$, n is the refractive index of the material. We can obtain $f = 83.06$ μm and $NA = 0.30$ ($D = 49.98$ μm, $h = 8.04$ μm and $n = 1.516$ for K9 glass), respectively. The obtained f and NA values were comparable to previously reported microlenses [40,41].

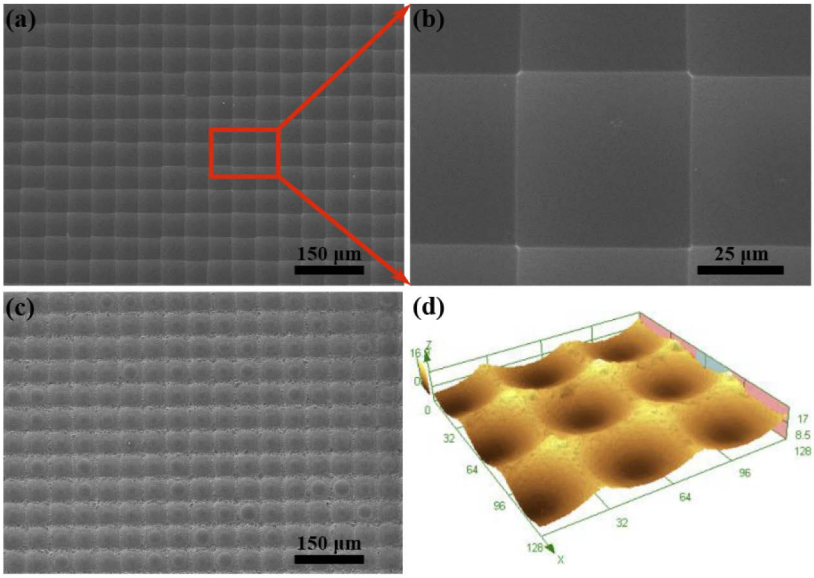

Fig. 2. Morphologies of different kinds of MLA. (a,b) SEM images of the smooth MLA. (c) SEM images of the micro/nano-structured MLA ($AD = 4$ μm). (d) 3D profile of the micro/nanoscale textured MLA.

3.2. Optical performance

The underwater imaging ability of the textured MLA was tested by a man-made optical imaging system. As shown in Fig. 3(a), the MLA and the imaging target were immersed in water and were put between an objective lens and a light source. For the object of a transparent letter "A", an array of miniaturized "A" was clearly captured by the CCD (Fig. 3(b)). In addition to the simple letter, more complex patterns such as "fish" can also be imaged through the structured MLA (Fig. 3(c)). The clear and uniform images of "A" and "fish" patterns demonstrate that the textured MLA has great imaging performance.

The image quality of the textured MLA can be quantitatively evaluated by the MTF, which is usually used to evaluate an optical imaging component [42]. In this experiment, the MTF of the textured MLA was calculated by the point spread function (PSF) of the captured image [43]. Figure 4(a) shows the experimental setup for measuring the PSF of the element. The incident light was spatially filtered by a pinhole (Thorlabs, P100D) with diameter of 100 μm and expanded through a microscope condenser. The collimated beam passing through the textured MLA was magnified by an objective lens (20×, NA = 0.40, Nikon) and was finally captured by a CCD camera chip. The PSF of the textured MLA was shown in Fig. 4(b), which was uniform in size and brightness. The MTF of a single microlens (e.g., in the red square of Fig. 4(b)) was calculated by the Fourier transform of the PSF and the result is shown in Fig. 4(c). The measured MTF value is over 0.6 at 55 lp/mm, indicating that the textured MLA exhibits excellent underwater imaging ability.

Although the resultant MLA with micro/nanoscale surface structure has poor imaging property in air, its imaging performance is outstanding in a water medium (Fig. 3). Once the sample was

Optics EXPRESS

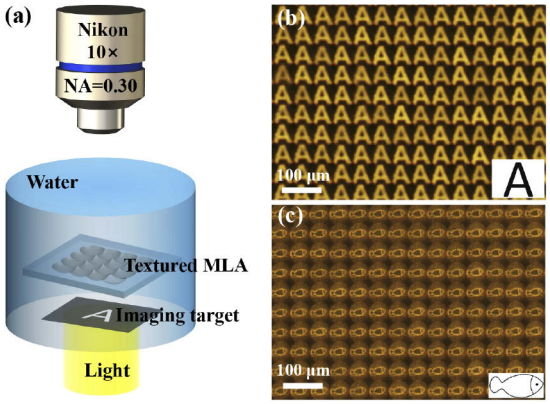

Fig. 3. Optical imaging performance of the resultant MLA. (a) Experimental setup of the underwater imaging system. (b,c) Images of an array of (b) letter "A" and (c) "fish" pattern captured through the textured MLA.

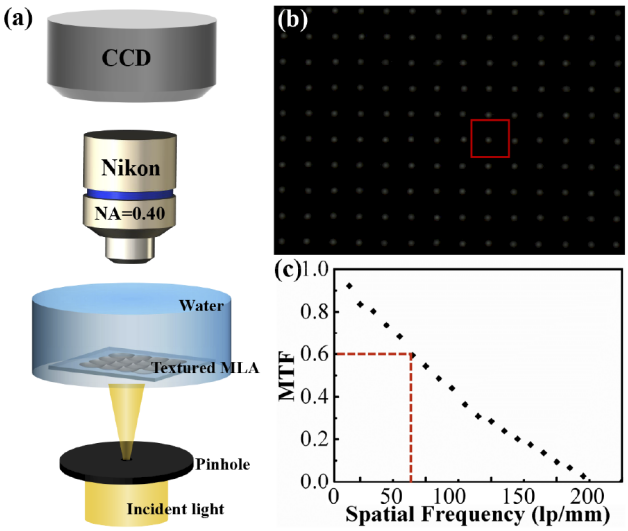

Fig. 4. (a) Schematic diagram of the experimental setup for measuring the PSF of the device. (b) The PSF of the textured MLA. (c) The calculated MTF of a single microlens.

immersed in water, the gap between the rough surface microstructures will be quickly occupied by water due to the superhydrophilicity of the laser-treated glass substrate. Because glass and water have comparable refractive index, a weaker scattering occurs when light passes through the glass/water interface [25,44]. Therefore, the fabricated micro/nanoscale structured-MLA has high imaging ability in underwater condition. Figure 5 shows the visible light transmittance of the smooth MLA and the textured MLA in water medium. Although the optical transmission of the textured MLA is lower than that of the smooth MLA, the laser-treated MLA still exhibits good transparence with the light transmittance higher than 68.7% at the wavelength of 600 nm, ensuring the high imaging ability of the laser-treated MLA.

Optics EXPRESS

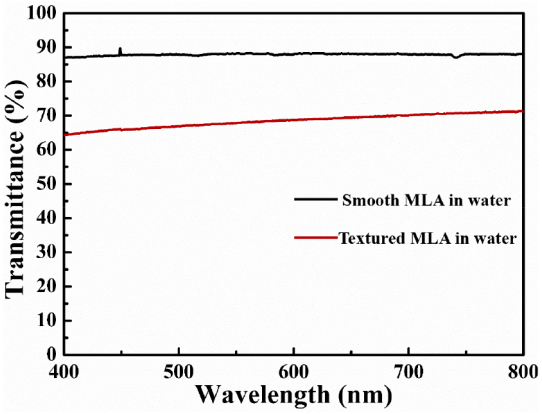

Fig. 5. Optical transmission spectrum of the smooth MLA and the textured MLA in water medium.

3.3. Underwater superoleophobicity

Glass is a typical inherently hydrophilic and oleophilic material. Water droplet on the smooth MLA has a water contact angle (WCA) of $46.1 \pm 1.1°$, while oil droplet on the smooth MLA has an oil contact angle (OCA) of $22.4 \pm 0.2°$. After the formation of micro/nanostructures, the resultant textured MLA shows superhydrophilicity with WCA of $7.8 \pm 1.3°$ and superoleophilicity with OCA of $2.5 \pm 0.1°$ in air. The underwater oil wettability of the MLAs was investigated by OCA and OSA measurements. When an oil droplet was placed on the textured MLA in water, the OCA was as large as $158.0 \pm 0.5°$, showing underwater superoleophobicity (Fig. 6(a)). As long as the textured MLA was slightly tilted, the oil droplet could easily roll away from the sample surface (Fig. 6(c)). The contact angle hysteresis was measured to be 2.0°. The low OSA value of $2.0 \pm 0.2°$ reveals that the underwater superoleophobic MLA exhibits ultralow adhesion to oils. By contrast, the smooth MLA without surface micro/nanostructures shows weak oleophobicity with an OCA of $102.5 \pm 0.3°$ in water (Fig. 6(b)), similar to the intrinsic underwater oleophobicity of the glass. Even if the smooth MLA was tilted at 90°, the oil droplet could still firmly adhere to the sample surface.

The excellent underwater superoleophobicity of the textured MLA surfaces is ascribed to the underwater Cassie wetting state [16,23,24]. The hydrophilicity of the glass substrate is enhanced by the laser-induced surface hierarchical micro/nanoscale structures on the textured MLA surface. Once the sample was immersed in water, the rough microstructures will be completely wetted by water. The trapped water layer around the surface microstructures only allows the oil droplet to sit on the solid/water interface, forming an oil/water/solid three-phase system (Fig. 6(d)). The trapped water is an ideal oil-repellent medium, which provides the repulsive force to oil, thereby endowing the textured MLA with underwater superoleophobicity and ultralow oil-adhesion. Figure 6(e) shows the OCAs and OSAs of the underwater oil droplets on the textured MLAs surfaces that ablated by laser at different *AD*s. It is shown that the surfaces can maintain underwater superoleophobicity (OCA > 150°) and extremely low oil-adhesion (OSA < 10°) as the *AD* increases from 2 μm to 14 μm. This result reveals that the anti-oil MLA can be prepared in a wide variation of processing parameters. As shown in Fig. 7, the textured MLA was demonstrated to show excellent underwater superoleophobicity to a wide range of oils, such as hexadecane, petroleum ether, decane, liquid paraffin and chloroform. These oil droplets could easily roll away once the sample was tilted a small angle (less than 10°).

Optics EXPRESS

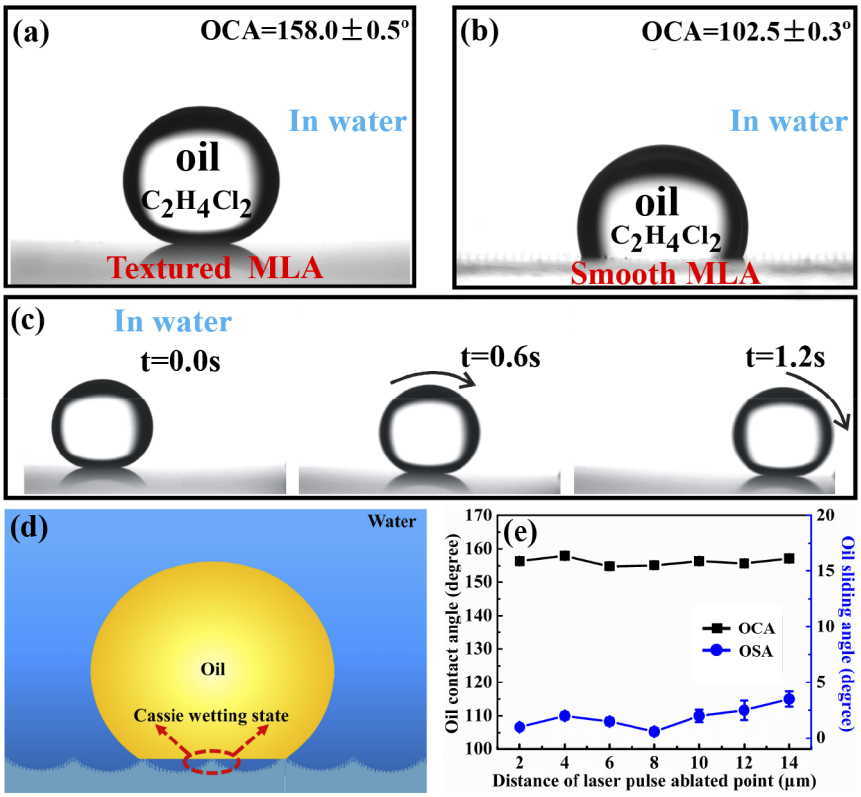

Fig. 6. Wettability of the fabricated MLAs. (a,b) Optical images of an oil droplet on different MLA surfaces in water: (a) textured MLA and (b) smooth MLA. (c) A 10 μL oil droplet sliding off the textured MLA surface with a tilting angle of 2° (see Visualization 1 for more details). (d) The contact model of an oil droplet on the micro/nano-structured MLA surface in water. (e) Relationship between the OCAs/OSAs and the *AD*.

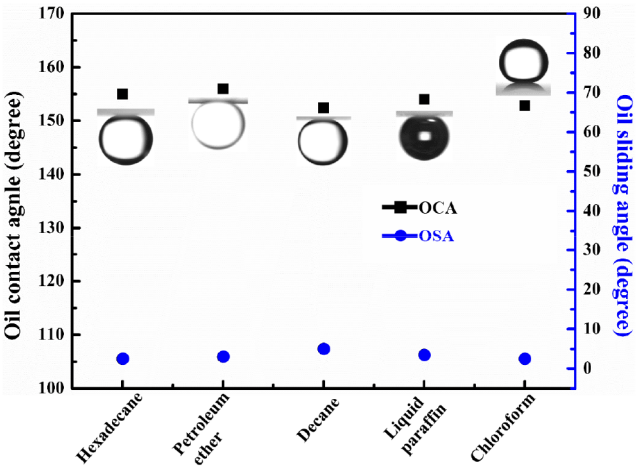

Fig. 7. Excellent underwater superoleophobicity and ultralow oil adhesion of the textured MLA (*AD* = 4 μm) to various oils.

Optics EXPRESS

3.4. Self-cleaning ability

The underwater superoleophobicity caused by the hierarchical micro/nanoscale structures can endow the textured MLA with anti-oil and self-cleaning ability in practical application. Figure 8(a) depicts the schematic illustration of self-cleaning ability of the textured MLA. A sesame oil droplet will quickly spread out when it is dripped onto the surface of the as-prepared micro/nano-structured MLA (Fig. 8(a)-1). Once the sample was immersed in water, the oil molecules in the rough surface structures will be quickly replaced by water (Fig. 8(a)-2). With the increase of water volume, all the oil contaminants will be cleaned without any residues. Most of oils are lighter than water, so the oil will float onto water surface (Fig. 8(a)-3). Figure 8(b) shows the result of dripping an oil-polluted superoleophobic MLA into water. Finally, the oil contaminant was completely removed from the MLA surface, showing remarkable self-cleaning property of the underwater superoleophobic MLA. The self-cleaning function was also verified from a top view (Fig. 8(c)). It can be seen that the surface of the MLA was so clean without any oil contamination (Fig. 8(c)-3). By contrast, when the same experiment was performed on the smooth MLA with weak underwater oleophobicity, many oil droplets remained on the MLA surface after cleaning process, which would seriously decrease the imaging performance. In addition, the textured MLA still maintained great underwater oil resistance after more than 20 cleaning cycles. These experiment results demonstrated that the textured MLA exhibits excellent oil resistance and self-cleaning ability.

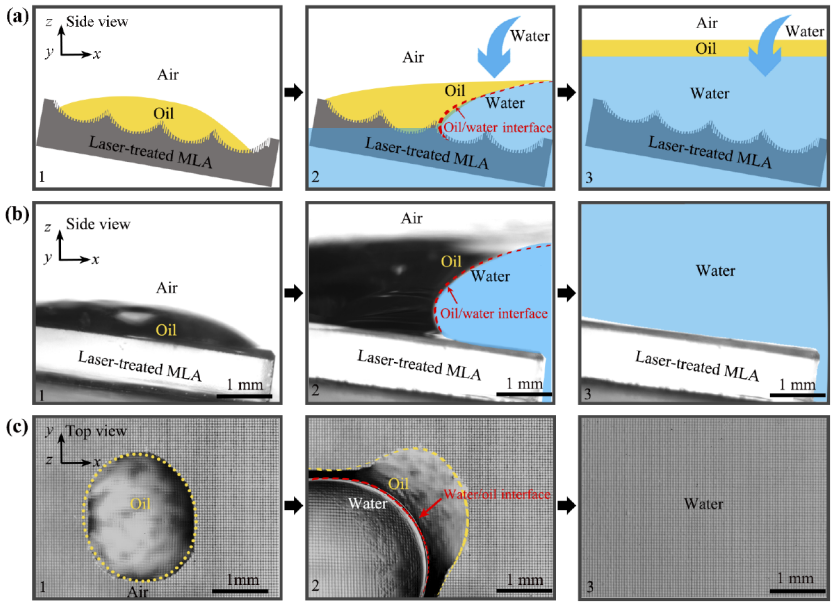

Fig. 8. Self-cleaning ability of the laser-treated MLA. (a) Schematic illustration of the self-cleaning process of the underwater superoleophobic MLA. (b) A series of digital photographs of dripping an oil-polluted superoleophobic MLA into water. (c) The top-view photographs of the self-cleaning process.

3.5. Durability

High durability is crucial for a MLA in practical applications. Figure 9(a) shows the OCA and OSA values of an oil droplet on the textured MLA that suffered from different cycles of sandpaper (800 mesh) abrasion. The sample was pulled to go forward for 15 cm for a cycle, with a load of 50 g. The result shows that the textured MLA remained underwater superoleophobicity and

Optics EXPRESS

ultralow oil-adhesion within 16 abrasion cycles. With further increasing the abrasion cycle, the OCA decreased and the OSA sharply increased to 90° due to the damage of the surface microstructures. The thermal stability was also investigated, as shown in Fig. 9(b). The OCAs of the oil droplet on the textured MLA surface maintained above 150° even though the MLA was heated at 130°C for an hour. Until the temperature was increased to 200°C, the textured MLA would loss underwater superoleophobicity. Therefore, the textured MLA has good abrasion resistance and thermal stability in addition to the excellent underwater superoleophobicity.

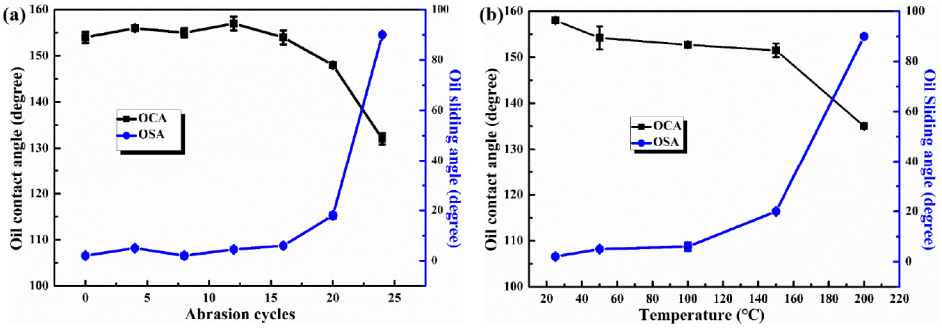

Fig. 9. Mechanical durability of the textured MLA. (a) Underwater oil wettability of the sample after different abrasion cycles. (b) Underwater oil wettability of the sample after heated at different temperature.

4. Conclusions

In conclusion, an underwater superoleophobic and anti-oil MLA was fabricated on the K9 glass substrate by FLWE and subsequent FLDW methods. The resultant microlenses have curved surface profile and their surfaces are decorated with micro/nanoscale structures. The MLA has great imaging ability in water. Clear and uniform image of complex patterns could be captured through the MLA. Compared to the normal MLA, the micro/nano-structured MLA also exhibits underwater superoleophobicity and ultralow oil-adhesion to a wide range of oils (e.g. 1,2-dichloroethane, hexadecane, petroleum ether, decane, liquid paraffin, and chloroform), which endows the MLA surface with great anti-oil ability. Underwater 1,2-dichloroethane oil droplet on the textured MLA has a contact angle of $158.0 \pm 0.5°$ and sliding angle of $2.0 \pm 0.2°$. Even though the MLA is polluted by oil contaminants, the MLA surface can be easily cleaned by water. In addition, the underwater superoleophobic MLA has good mechanical durability. We believe that the novel superoleophobic and anti-oil MLA will have broad applications in bioscience research, ocean exploration, and underwater optical imaging.

Funding

National Natural Science Foundation of China (61435005, 61805192, 61875158, U1630111); National Key Research and Development Program of China (2017YFB1104700).

Acknowledgments

We thank the Collaborative Innovation Center of Suzhou Nano Science and Technology and the Instrument Analysis Center of Xi'an Jiaotong University. The SEM work was done at the International Center for Dielectric Research (ICDR), Xi'an Jiaotong University.

Optics EXPRESS

Disclosures

The authors declare no conflicts of interest.

References

1. Y. M. Song, Y. Xie, V. Malyarchuk, J. Xiao, I. Jung, K. Choi, Z. Liu, H. Park, C. Lu, R. Kim, R. Li, K. B. Crozier, Y. Huang, and J. A. Rogers, "Digital Cameras with Designs Inspired by the Arthropod Eye," Nature **497**(7447), 95–99 (2013).
2. P. Gorzelak, M. A. Salamon, R. Lach, M. Loba, and B. Ferre, "Microlens Arrays in the Complex Visual System of Cretaceous Echinoderms," Nat. Commun. **5**(1), 3576 (2014).
3. Y. Wei, Q. Yang, H. Bian, F. Chen, M. Li, Y. Dai, and X. Hou, "Fabrication of High Integrated Microlens Arrays on a Glass Substrate for 3D Micro-Optical Systems," Appl. Surf. Sci. **457**, 1202–1207 (2018).
4. X. Li, X. Li, J. Shao, H. Tian, C. Jiang, Y. Luo, L. Wang, and Y. Ding, "Shape-Controllable Plano-Convex Lenses with Enhanced Transmittance via Electrowetting on a Nanotextured Dielectric," J. Mater. Chem. C **4**(39), 9162–9166 (2016).
5. C. Lv, H. Xia, W. Guan, Y. Sun, Z. Tian, T. Jiang, Y. Wang, Y. Zhang, Q. Chen, K. Ariga, Y. Yu, and H. Sun, "Integrated Optofluidic-Microfluidic Twin Channels: toward Diverse Application of Lab-on-a-Chip Systems," Sci. Rep. **6**(1), 19801 (2016).
6. V. Vespini, S. Coppola, M. Todino, M. Paturzo, V. Bianco, S. Grilli, and P. Ferraro, "Forward Electrohydrodynamic Inkjet Printing of Optical Microlenses on Microfluidic Devices," Lab Chip **16**(2), 326–333 (2016).
7. E. Wrzesniewski, S. Eom, W. Cao, W. T. Hammond, S. Lee, E. P. Douglas, and J. Xue, "Enhancing Light Extraction in Top-Emitting Organic Light-Emitting Devices Using Molded Transparent Polymer Microlens Arrays," Small **8**(17), 2647–2651 (2012).
8. Q. Cheng, M. Li, Y. Zheng, B. Su, S. Wang, and L. Jiang, "Janus Interface Materials: Superhydrophobic Air/Solid Interface and Superoleophobic Water/Solid Interface Inspired by a Lotus Leaf," Soft Matter **7**(13), 5948–5951 (2011).
9. Z. Cheng, H. Lai, Y. Du, K. Fu, R. Hou, C. Li, N. Zhang, and K. Sun, "pH-Induced Reversible Wetting Transition between the Underwater Superoleophilicity and Superoleophobicity," ACS Appl. Mater. Interfaces **6**(1), 636–641 (2014).
10. Z. Cheng, H. Liu, H. Lai, Y. Du, K. Fu, C. Li, J. Yu, N. Zhang, and K. Sun, "Regulating Underwater Oil Adhesion on Superoleophobic Copper Films through Assembling N-Alkanoic Acids," ACS Appl. Mater. Interfaces **7**(36), 20410–20417 (2015).
11. J. Huo, Q. Yang, F. Chen, J. Yong, Y. Fang, J. Zhang, L. Liu, and X. Hou, "Underwater Transparent Miniature "Mechanical Hand" Based on Femtosecond Laser-Induced Controllable Oil-Adhesive Patterned Glass for Oil Droplet Manipulation," Langmuir **33**(15), 3659–3665 (2017).
12. J. Yong, F. Chen, Q. Yang, J. Huo, and X. Hou, "Superoleophobic Surfaces," Chem. Soc. Rev. **46**(14), 4168–4217 (2017).
13. K. Li, J. Ju, Z. Xue, J. Ma, L. Feng, S. Gao, and L. Jiang, "Structured Cone Arrays for Continuous and Effective Collection of Micron-Sized Oil Droplets from Water," Nat. Commun. **4**(1), 2276 (2013).
14. L. Li, Z. Liu, Q. Zhang, C. Meng, T. Zhang, and J. Zhai, "Underwater Superoleophobic Porous Membrane Based on Hierarchical TiO2 Nanotubes: Multifunctional Integration of Oil-Water Separation, Flow-through Photocatalysis and Self-Cleaning," J. Mater. Chem. A **3**(3), 1279–1286 (2015).
15. D. Wu, S. Wu, Q. Chen, S. Zhao, H. Zhang, J. Jiao, J. A. Piersol, J. Wang, H. B. Sun, and L. Jiang, "Facile Creation of Hierarchical PDMS Microstructures with Extreme Underwater Superoleophobicity for Anti-Oil Application in Microfluidic Channels," Lab Chip **11**(22), 3873–3879 (2011).
16. M. Liu, S. Wang, Z. Wei, Y. Song, and L. Jiang, "Bioinspired Design of a Superoleophobic and Low Adhesive Water/Solid Interface," Adv. Mater. **21**(6), 665–669 (2009).
17. X. Liu, J. Zhou, Z. Xue, J. Gao, J. Meng, S. Wang, and L. Jiang, "Clam's Shell Inspired High-Energy Inorganic Coatings with Underwater Low Adhesive Superoleophobicity," Adv. Mater. **24**(25), 3401–3405 (2012).
18. E. Zhang, Z. Cheng, T. Lv, L. Li, and Y. Liu, "The Design of Underwater Superoleophobic Ni/NiO Microstructures with Tunable Oil Adhesion," Nanoscale **7**(45), 19293–19299 (2015).
19. L. Xu, J. Peng, Y. Liu, Y. Wen, X. Zhang, L. Jiang, and S. Wang, "Nacre-Inspired Design of Mechanical Stable Coating with Underwater Superoleophobicity," ACS Nano **7**(6), 5077–5083 (2013).
20. J. Rombaut, R. A. Maniyara, R. A. Bellman, D. F. Acquard, A. S. Baca, J. Osmond, W. Senaratne, M. A. Quesada, D. Baker, P. Mazumder, and V. Pruneri, "Antireflective Transparent Oleophobic Surfaces by Noninteracting Cavities," ACS Appl. Mater. Interfaces **10**(49), 43230–43235 (2018).
21. H. Wang and Z. Guo, "Design of Underwater Superoleophobic TiO2 Coatings with Additional Photo-Induced Self-Cleaning Properties by One-Step Route Bio-Inspired from Fish Scales," Appl. Phys. Lett. **104**(18), 183703 (2014).
22. Z. Wang, L. Zhu, W. Li, and H. Liu, "Bioinspired in Situ Growth of Conversion Films with Underwater Superoleophobicity and Excellent Self-Cleaning Performance," ACS Appl. Mater. Interfaces **5**(21), 10904–10911 (2013).
23. Z. Xue, Y. Cao, N. Liu, L. Feng, and L. Jiang, "Special Wettable Materials for Oil/Water Separation," J. Mater. Chem. A **2**(8), 2445–2460 (2014).

Optics EXPRESS

24. Z. Xue, M. Liu, and L. Jiang, "Recent Developments in Polymeric Superoleophobic Surfaces," J. Polym. Sci., Part B: Polym. Phys. **50**(17), 1209–1224 (2012).
25. J. Yong, F. Chen, Q. Yang, G. Du, C. Shan, H. Bian, U. Farooq, and X. Hou, "Bioinspired Transparent Underwater Superoleophobic and Anti-Oil Surfaces," J. Mater. Chem. A **3**(18), 9379–9384 (2015).
26. J. Yong, F. Chen, Q. Yang, and X. Hou, "Femtosecond Laser Controlled Wettability of Solid Surfaces," Soft Matter **11**(46), 8897–8906 (2015).
27. J. Yong, F. Chen, Q. Yang, D. Zhang, U. Farooq, G. Du, and X. Hou, "Bioinspired Underwater Superoleophobic Surface with Ultralow Oil-Adhesion Achieved by Femtosecond Laser Microfabrication," J. Mater. Chem. A **2**(23), 8790–8795 (2014).
28. Z. Wang, X. Jiang, X. Cheng, C. H. Lau, and L. Shao, "Mussel-Inspired Hybrid Coatings that Transform Membrane Hydrophobicity into High Hydrophilicity and Underwater Superoleophobicity for Oil-in Water Emulsion Separation," ACS Appl. Mater. Interfaces **7**(18), 9534–9545 (2015).
29. F. Zhang, W. Zhang, Z. Shi, D. Wang, J. Jin, and L. Jiang, "Nanowire-Haired Inorganic Membranes with Superhydrophilicity and Underwater Ultralow Adhesive Superoleophobicity for High-Efficiency Oil/Water Separation," Adv. Mater. **25**(30), 4192–4198 (2013).
30. L. Zhang, Y. Zhong, D. K. Cha, and P. Wang, "Self-Cleaning Underwater Superoleophobic Mesh for Oil-Water Separation," Sci. Rep. **3**(1), 2326 (2013).
31. M. Zhang, T. Zhang, and T. Cui, "Wettability Conversion from Superoleophobic to Superhydrophilic on Titania/Single-Walled Carbon Nanotube Composite Coatings," Langmuir **27**(15), 9295–9301 (2011).
32. J. L. Yong, S. C. Singh, Z. Zhan, F. Chen, and C. Guo, "Substrate-Independent, Fast, and Reversible Switching between Underwater Superaerophobicity and Aerophilicity on the Femtosecond Laser-Induced Superhydrophobic Surfaces for Selectively Repelling or Capturing Bubbles in Water," ACS Appl. Mater. Interfaces **11**(8), 8667–8675 (2019).
33. J. L. Yong, F. Chen, M. Li, Q. Yang, Y. Fang, J. Huo, and X. Hou, "Remarkably Simple Achievement of Superhydrophobicity, Superhydrophilicity, Underwater Superoleophobicity, Underwater Superoleophilicity, Underwater Superaerophobicity, and Underwater Superaerophilicity on Femtosecond Laser Ablated PDMS Surfaces," J. Mater. Chem. A **5**(48), 25249–25257 (2017).
34. J. L. Yong, Q. Yang, F. Chen, D. Zhang, U. Farooq, G. Du, and X. Hou, "A Simple Way to Achieve Superhydrophobicity, Controllable Water Adhesion, Anisotropic Sliding, and Anisotropic Wetting Based on Femtosecond-Laser-Induced Line-Patterned Surfaces," J. Mater. Chem. A **2**(15), 5499–5507 (2014).
35. F. Chen, H. Liu, Q. Yang, X. Wang, C. Hou, H. Bian, W. Liang, J. Si, and X. Hou, "Maskless Fabrication of Concave Microlens Arrays on Silica Glasses by a Femtosecond-Laser-Enhanced Local Wet Etching Method," Opt. Express **18**(19), 20334–20343 (2010).
36. H. Liu, H. Bian, F. Chen, Q. Yang, P. Qu, G. Du, J. Si, X. Wang, and X. Hou, "Versatile Route to Gapless Microlens Arrays Using Laser-Tunable Wet-Etched Curved Surface," Opt. Express **20**(12), 12939–12948 (2012).
37. J. L. Yong, S. C. Singh, Z. Zhan, E. Mohamed, F. Chen, and C. Guo, "Femtosecond Laser-Produced Underwater "Superpolymphobic" Nanorippled Surfaces: Repelling Liquid Polymers in Water for Application of Controlling Polymer Shape and Adhesion," *ACS Appl. Nano Mater.* doi.org/10.1021/acsanm.9b01869 (2019).
38. X. Bai, Q. Yang, Y. Fang, J. Zhang, J. Yong, X. Hou, and F. Chen, "Superhydrophobicity-Memory Surfaces Prepared by a Femtosecond Laser," *Chem. Eng. J.* doi.org/10.1016/j.cej.2019.123143 (2019).
39. M. Li, Q. Yang, F. Chen, J. Yong, H. Bian, Y. Wei, Y. Fang, and X. Hou, "Integration of Great Water Repellence and Imaging Performance on a Superhydrophobic PDMS Microlens Array by Femtosecond Laser Microfabrication," Adv. Eng. Mater. **21**(3), 1800994 (2019).
40. Q. Xu, B. Dai, Y. Huang, H. Wang, Z. Yang, K. Wang, S. Zhuang, and D. Zhang, "Fabrication of Polymer Microlens Array with Controllable Focal Length by Modifying Surface Wettability," Opt. Express **26**(4), 4172–4182 (2018).
41. S. Tong, H. Bian, Q. Yang, F. Chen, Z. Deng, J. Si, and X. Hou, "Large-Scale High Quality Glass Microlens Arrays Fabricated by Laser Enhanced Wet Etching," Opt. Express **22**(23), 29283–29291 (2014).
42. J. C. Feltz and M. A. Karim, "Modulation Transfer Function of Charge-Coupled Devices," Appl. Opt. **29**(5), 717–722 (1990).
43. A. Brückner, J. Duparré, R. Leitel, P. Dannberg, A. Bräuer, and A. Tünnermann, "Thin Wafer-Level Camera Lenses Inspired by Insect Compound Eyes," Opt. Express **18**(24), 24379–24394 (2010).
44. S. Haghanifar, T. Gao, R. T. R. D. Vecchis, B. Pafchek, T. D. B. Jacobs, and P. W. Leu, "Ultrahigh-Transparency, Ultrahigh-haze Nanograss Glass with Fluid-Induced Switchable Haze," Optica **4**(12), 1522–1525 (2017).